

Rendering human skin using a multi-layer reflection model

Ling Li and Carmen So-ling Ng

Abstract: - A key element to creating realistic images is the appearance of surfaces. In order to overcome the artificial look of synthetic humans, human skin has to be modelled in all its variety. A new physically-based skin reflection model is presented in this paper to render a diverse selection of skin complexions. The reflection model is based on steady-state light transport theory in multi-layered skin tissue. A three-layer simulation model has been developed to capture the effect of natural sebum on skin appearance. Sebum is found over most parts of the body, causing skin to look more specular, depending on the viewing conditions. Optical and geometric properties are used as control parameters to influence the surface reflection and subsurface scattering of light within the three layers. The resultant reflection consists of the specular reflection due to the Fresnel effect, as well as the diffuse reflection from subsurface scattering. The Monte Carlo method is used to simulate the propagation of light in skin tissue. Various effects like scattering, absorption, reflection and transmission have been taken into account. The bi-directional reflectance distribution function (BRDF) obtained from the simulation is used to render the appearance of human skin. Comparisons between the simulated BRDF results and experimental measurements show that the physical simulation is highly realistic.

Keywords: - skin optics, subsurface scattering, Multi-layer reflection, light transport

1. INTRODUCTION

One of the greatest challenges posed to the graphics community is to create a computer generated human so real that it cannot be distinguished from the real life character. Realistic rendering of human skin helps in application such as the facial expression and gesture understanding and detections [1]. It could also form the basis for dermatological diagnosis [2]. Besides the immense variety in skin tones, textures and physical characteristics, the fact that our highly tuned visual system could detect any slight discrepancy in the synthetic human character compounds the difficulty of creating a convincingly real human figure. To intuitively sculpt and paint a synthetic figure requires not only a strong artistic sense and keen observation, but also a great amount of time and effort to achieve acceptable realism. Common techniques used by computer graphics artists to simulate skin texture include diffuse and specular mapping for three-dimensional

highlights as well photorealistic texture mapping. The effects are obtained intuitively through visual observation and experimentation with different lighting, image maps and colours to arrive at the final scene. This ad hoc process not only requires a great amount of time and technical effort, but a strong artistic sense as well, to achieve acceptable realism. In this project, we aim to automate this process by creating physically-based reflection models that can be used to render most types of skin.

The synthesis of realistic human skin appearance is one of the most important steps towards rendering a convincing digital human character. Human skin has an immense variety in colour, reflectance and texture, which are dependent on race, gender, age and other physical conditions. The underlying optical behaviour, however, can be modelled for all skin types, as principles of light transport in skin are well established from research work done in the biomedical field. For example, Gemert and Jacques et al have done an excellent analysis of skin optics [3].

A physically-based skin reflection model is presented in this work, which explicitly models the material's optical properties and the propagation and scattering of light within the material. This phenomenon, known as subsurface scattering, is common in organic materials as well as plastics and other composite materials. Most reflection models are not suitable for dielectric organic materials because they often do not take into account subsurface scattering. Subsurface scattering within the material contributes significantly to diffuse reflection of dielectric materials but is neglected in most reflection models. Subsurface scattering is especially important in organic materials since they are translucent and contain a high percentage of water. Reflectance for such materials is dominated by subsurface diffuse component at near perpendicular angles of incidence and Fresnel surface reflections at glancing angles.

In subsurface scattering, light enters a material and is scattered, transmitted and absorbed by the constituents in the medium. The scattered light may exit the medium in random directions and appear as reflected light to the observer. The theory of scattering in layered media was originally developed to explain the transport of heat and light by radiation in planetary and solar atmospheres. It has recently

Manuscript received ????, ?????

Revised version received ???????

Ling Li is with the Department of Computing at Curtin University of Technology, Australia.

Carmen So-ling Ng is with the School of Computer Engineering, at Nanyang Technological University, Singapore.

Contact: L.Li@curtin.edu.au

been adopted by graphics researchers to simulate the appearance of paint, human skin, and organic leaves, etc.

The reflection model of human skin depends on the optical properties of its structural components. To capture the differences in appearance caused by the presence of sebum on skin surface, we have developed a new three-layer simulation model. The influence of the sebum layer on the surface reflectance of human skin is often neglected in other skin reflection models. The modelling of the sebum layer is emphasised in this work as it makes skin appear more natural and real. Our approach is highly flexible as the model is controlled by physical parameters that can be varied to render a wide variety of skin types and other similar multi-layered surfaces.

The applications of the simulation presented here can be extended to many other fields, including physics, engineering and biomedical research, where the accuracy of physically based models is essential. In the treatment of skin disorders for example, information on the propagation of laser light in skin layers related to its optical properties is required for diagnosis and treatment.

2. PREVIOUS WORK

Reflectance data can either be measured directly or obtained from theoretical simulations. The reflective behaviour of a surface is often represented as a function of incident and reflected light directions in a bi-directional reflectance distribution function (BRDF).

Specialised mechanisms known as gonioreflectometers that position a light source and a detector at various directions from a flat sample of the material, are traditionally used to measure the reflection model directly. Dana et al [4] have acquired the reflectance of a human skin sample, classified as sample 39 of the Columbia-Utrecht Reflectance and Texture Database, which is publicly available on the Internet. The skin was removed from the cadaver and prepared into a flat sample, mounted in a positioning device to ensure stability for the time needed to gather the BRDF information. Marschner et al [5] have taken a different approach by making use of the natural curvature of the human form to present different angles to the imaging detector simultaneously, extracting valid BRDFs from living human skin.

Reflection models based on measurements are difficult to obtain since up to five dimensions have to be acquired, involving a large number of angles and wavelengths. Measuring a full BRDF for skin may take several hours even with the use of expensive equipment. There are also problems with light source and camera stability, with variations in surface geometry and interreflections on the surface.

Theoretical models, on the other hand, are based on the geometric and optical properties of the material. They provide quantitative values that have shown to be in good approximation of experimental data. Moreover, they can be adapted to applications where physically based rendering or simulation accuracy is essential.

Most research work on theoretical models concentrates on improving specular reflection on rough surfaces using

geometric optics. Diffuse reflection is often approximated using the Lambert's Cosine Law. He et al [6] derived an isotropic reflection model based on physical optics, which consists of an ideal diffuse component, a directional-diffuse component and a specular mirror component, expressed by a set of analytic expressions. Oren and Nayar [7] modelled the surface as a collection of Lambertian facets and accounts for complex geometric and radiometric phenomena such as masking, shadowing and interreflections between facets.

Another approach is to perform a deterministic or Monte Carlo simulation on a surface at micro scale. Hanrahan [8] presented a model for subsurface scattering in layered surfaces based on one-dimensional transport theory. The experiments are based on measured values and they do not claim to have an experimentally verified model.

In the field of skin cancer research, Wang et al [9] developed a Monte Carlo model of steady-state light transport in multi-layered tissue. Their model deals only with the transport of a perpendicularly incident narrow photon beam. To obtain the reflection model as a function of both incident and reflection angles, this simplification has to be removed.

We present a framework for rendering human skin based on skin optics principles and subsurface scattering. Unlike Hanrahan's work [8], which has not been experimentally verified, we have compared our simulation results with measured reflectance data from the Columbia-Utrecht Reflectance Database [4] and Marschner et al [5], and found them to be highly similar. A layer of sebum has been included in the physically-based three-layer skin reflection model.

3. SKIN OPTICS

Physically based simulations of light transport require some detailed knowledge of the geometric and optical properties of layers in the material. When a beam of light reaches the skin surface, it will either be specularly reflected by the epidermis surface or refracted and transmitted into the skin. Surface specular reflection is approximately 5% of the incident light, as governed by the Fresnel equations. The amount of specular reflection varies with the amount of facial oil or sebum found on the surface of the skin, and is independent of wavelength. The Fresnel reflection coefficients for a refractive index of 1.43 are shown in Figure 1. They can be efficiently computed using Schlick's approximation [10].

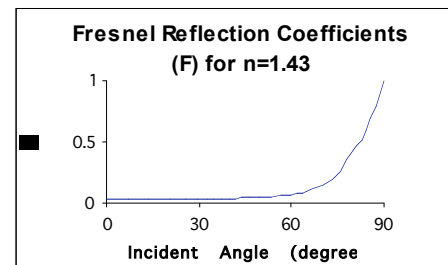


Figure 1. Fresnel Reflection Coefficients

The remaining light enters the tissue where it is attenuated by absorption and scattering. Scattered photons propagate in random directions described by the phase function. These photons contribute to the diffuse distribution of light in the tissue that extends beyond the boundaries of the collimated incident beam. Internal reflection occurs when backscattered photons reach the tissue-air boundary at an angle greater than the critical angle of reflection.

The scattering phase function expresses the probability density function that a photon moving in a certain direction is scattered into another direction. Individual layers of skin demonstrate strong forward scattering. Available experimental data of skin layers have shown that their phase functions can be represented quite reasonably by the Henyey-Greenstein phase function [3]. The Henyey-Greenstein function, P_{HG} , produces an ellipse with eccentricity g and one focus at the origin:

$$P_{HG}(g, a) = \frac{1 - g^2}{(1 - 2ga + g^2)^{1.5}} \quad (1)$$

where a is the cosine of the deflection angle and g is the anisotropy factor, $g \in (-1, 1)$. A value of 0 indicates isotropic scattering and a value near 1 indicates strong forward scattering. Values of g range from 0.3 to 0.98 for human tissues.

Based on the probability function, the choice of a can be expressed as a function of the random number ξ as follows:

$$a = \begin{cases} \frac{1}{2g} \left\{ 1 + g^2 \left[\frac{1 - g^2}{1 - g + 2g\xi} \right]^2 \right\} & \text{if } g > 0 \\ 2\xi - 1 & \text{if } g = 0 \end{cases} \quad (2)$$

After multiple scattering, some of the transmitted light will re-emerge through the air-skin interface into the air. The re-emergence of light will result in the observed diffuse reflection. The amount of diffuse reflection is determined by both the scattering and absorption properties of the skin tissue. The stronger the absorption, the less the diffuse reflection; the stronger the scattering, the larger the diffuse reflection [11].

4. APPEARANCE OF SEBUM-COVERED SKIN

Technically, human skin consists of three layers with almost homogeneous properties: the epidermis (top layer), the dermis (middle layer) and the subcutis (bottom layer). The subcutis is the deepest layer, consisting mainly of adipose or fatty tissues and has been excluded in this simplified skin model, as shown in Figure 2, as this layer does not contribute significantly to the exterior reflectance of the skin.

Homogeneity in the thickness of the skin layers as well as in the distribution of melanin and blood are some of the

simplifying assumptions made in this model. To the best of the author's knowledge, there are currently no actual measurements of the different thickness and optical properties of skin from different parts of the body. Hence, any attempts to vary these properties are at best ad hoc.

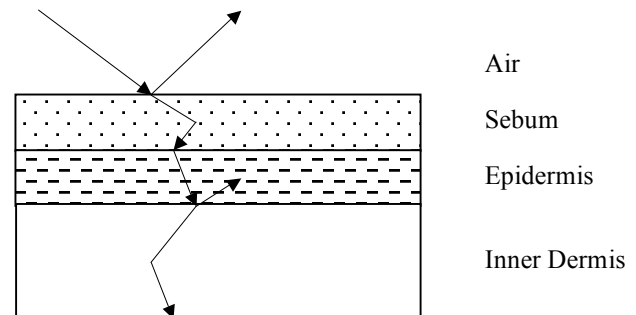


Figure 2. Light propagation in a three-layer skin model

The layers are assumed to have the same refractive index (approximately 1.37 to 1.5), but with different number of absorbers and scatterers randomly distributed within [GEM89]. Wavelength dependent absorption and scattering coefficients can be assigned to both the epidermis and dermis. The anisotropy for skin tissue, g , defined as the mean cosine of the deflection angle due to a scattering event, has typical values in the range of 0.7-0.95 [12].

The epidermis is the thinnest layer and is at maximum 1 mm. It contains pigment particles called melanin that act as wavelength dependent absorbers and strong forward scatterers. Melanin particles cause a brown-black coloration as their density increases, and scatters strongly in the forward direction. Based on the approximation by Jacques [12], the net epidermal absorption coefficient, $\sigma_{a,epi}$ for a moderately pigmented adult will have the absorption coefficients listed below in Table 1:

Table 1. Absorption coefficients of epidermis in the visible spectrum

Wavelength [nm]	470 (blue)	550 (green)	656 (red)
$\sigma_{a,epi}$ [cm ⁻¹]	85	50	28

The scattering coefficients of the epidermis are close to the scattering coefficients of the dermis (Refer to Table 2), although they are of minor importance due to the thinness of the epidermis.

The dermis is approximately 2.5 mm thick. It is a thick layer of weakly absorbing and strongly scattering connective tissues and blood. Blood may be either explicitly taken into account or it may be assumed to be homogeneously distributed in the dermis. It contains ingredients such as haemoglobin, bilirubin and beta-carotene, which scatters light isotropically and has strong absorption for the green and blue parts of the spectrum, producing the pinkish tint on skin [7].

Research has revealed that individual layers of skin show strong forward scattering [3]. The optical properties of the dermis are basically the same for all ethnic races [13]. According to the approximation proposed by Jacques [12], the dermal scattering and absorption coefficients $\sigma_{s, \text{derm}}$ and $\sigma_{a, \text{derm}}$ are listed in Table 2.

Table 2. Scattering and absorption coefficients of dermis in the visible spectrum

Wavelength [nm]	470 (blue)	550 (green)	56 (red)
$\sigma_{a, \text{derm}}$ [cm ⁻¹]	6	7	0.58
$\sigma_{s, \text{derm}}$ [cm ⁻¹]	60	37	23

The oil found on the skin surface is a complex mixture of sebum, lipids and sweat. Sebum is produced by sebaceous glands that are found over most parts of the human body. The main functions of sebum are to lubricate and waterproof skin, and to protect the skin from harmful bacteria. Sebum

production varies with age, gender and race. Adult males generally produce more sebum than adult females because they secrete higher level of androgens. Sebum production declines with age. Black facial skin has higher hydration, elasticity and sebum production than white skin.

When light first strikes the skin, it is reflected by the flat, oily cells of the epidermis. Sebum smoothes out the roughness of the skin surface, causing it to look shinier and more specular due to the smooth air-sebum interface. The refractive index for the thin sebum layer is higher than that of the epidermis; it is assigned a value of 1.5. A higher refractive index increases the amount of light reflected off the air-sebum interface. Fresnel reflectance increases with refractive index, as shown in Figure 3. Surface specular reflectance is approximately 4% of the incident light at perpendicular angles of incidence. At near grazing angles, Fresnel reflection is almost 100%. Fresnel reflectance coefficients can be efficiently computed using Schlick's approximation [10].

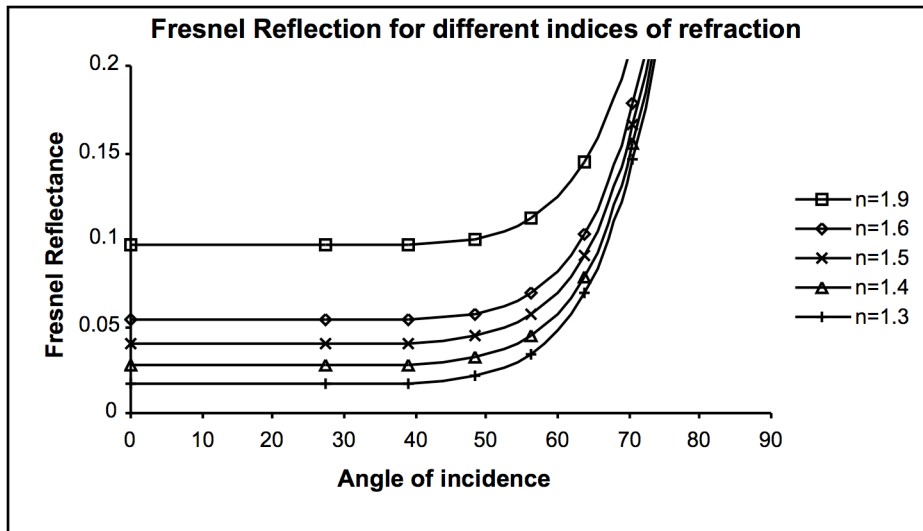


Figure 3. Effect of Refractive Index (n) on Fresnel reflection

4. TRANSPORT OF LIGHT IN SKIN

Equations can be derived to describe the transport and measurement of light energy in human skin. The light transport equation is normally written as a linear integral-differential equation of radiative transfer [8]:

$$\cos \theta \frac{\partial L(\theta, \phi)}{\partial z} = -m_t L(\theta, \phi) + m_s \int p(z, \theta, \phi; \theta', \phi') L(\theta', \phi') d\theta' d\phi' \quad (3)$$

where

- (θ, ϕ) : Angles of incidence
- (θ', ϕ') : Angles of reflection
- $L(\theta, \phi)$: Incoming radiance
- $p(z, \theta, \phi; \theta', \phi')$: Scattering phase function
- m_t : Interaction coefficient ($m_t = m_a + m_s$)

The above equation accounts for the balance of energy within a differential volume element. It describes the change in light energy along an infinitesimal direction dz . The first component accounts for the radiance lost through scattering and absorption. The second component accounts for the radiance scattered in the direction of dz from all incoming directions.

It is assumed that all quantities depend on z and not on x and y directions. This simplification is valid if the incoming radiance is constant over the region. All our terms have been written without the specificity of wavelength, assuming linearity with respect to wavelengths for simplicity.

To solve the equation, it can be converted into an equivalent double intergral equation as follows:

$$L(z; \theta, \phi) = \int_0^z e^{-\int_0^z m_t \frac{dz'}{\cos \theta}} \int m_s(z') p(z'; \theta, \phi, \theta', \phi') d\omega' \frac{dz'}{\cos \theta} \quad (4)$$

Generally, this kind of equation cannot be solved analytically. Monte Carlo simulation of photon propagation offers a flexible yet rigorous approach to solving light transport. It describes local rules of propagation that are expressed as probability distributions derived from the interaction coefficients and phase function, which determine the step size and direction of photons at each scattering event.

5. MONTE CARLO MODEL OF LIGHT PROPOGATION

Light is treated as streams of photons and not as a wave phenomenon in Monte Carlo simulations. Thus, features such as phase change and polarisation are ignored. Photon rays are generated from a light source to the scene, tracked from interaction with the skin surface, scattered through multiple layers until the ray is either absorbed or reflected from the skin surface as diffuse reflection.

Monte Carlo simulation is performed by tracing individual photon histories [14]. Rays are generated from the light source to the scene, and tracked from interaction with the surface boundary, through the skin layers, until the ray is absorbed or reflected away from the skin surface. A random number generator is used to sample discrete events from probability distributions derived from the interaction coefficients and phase function.

In our work, we have adapted and modified the algorithm presented by Wang and Jacques [9], which was originally intended for the medical research of steady-state light transport in multi-layered tissue. The Monte Carlo simulation described in their paper deals with the transport of an infinitely narrow photon beam that is *perpendicularly* incident on a multi-layered tissue. We have removed this simplification and taken into account photon beams coming from a wide array of angles in order to obtain the full BRDF as a function of the angle of incidence and viewing angle, for integration into a rendering system. We are mainly interested in obtaining diffuse reflection from subsurface scattering in a three-layer skin model, although other physical quantities like photon absorption, fluence and transmission can be obtained as well.

Each photon packet is initially assigned a weight, W , equal to unity. The photon is then projected into the tissue. When it hits the tissue surface, a mismatch in refractive indices causes specular reflection to occur. Assuming perpendicularly incident collimated light, if the refractive indices of the outside medium and sebum layer are n_1 and n_2 respectively, then the specular reflectance, $R_{sp}(0)$ is specified as:

$$R_{sp}(0) = \frac{(n_1 - n_2)^2}{(n_1 + n_2)^2} \tag{5}$$

For all other angles of incidence, Schlick's approximation is used to obtain the Fresnel reflection factor. [10]

The step size of the photon packet is calculated based on the sampling of the probability function for the photon's free path $s \in [0, \infty)$. To derive the step size of the photon packet,

we start with the interaction coefficient σ_t , which is defined as the probability of interaction per unit length in the step interval $(s', s'+ds')$:

$$\sigma_t = \frac{-dP\{s \geq s' \}}{P\{s \geq s' \} ds'} \tag{6}$$

or rearranged as:

$$d(\ln(P\{s \geq s' \})) = -\sigma_t ds' \tag{7}$$

After integration over s' in the range $(0, s)$, the following exponential distribution can be obtained:

$$P\{s \geq s_1\} = \exp(-\sigma_t s_1) \tag{8}$$

This equation can be rearranged to yield the following cumulative distribution function of free path s :

$$P\{s < s_1\} = 1 - \exp(-\sigma_t s_1) \tag{9}$$

The cumulative distribution function can be assigned to the uniformly distributed random number ξ and rearranged to arrive at the step size:

$$s_1 = \frac{-\ln(1 - \xi)}{\sigma_t} \tag{10}$$

Substituting the random number ξ with $(1-\xi)$:

$$s_1 = \frac{-\ln(\xi)}{\sigma_t} \tag{11}$$

s_1 gives a mean free path between interaction sites of $1/\sigma_t$ because the statistical average of $-\ln(\xi)$ is 1.

After taking a step, the photon weight will be attenuated due to some absorption at the interaction site. A fraction of the photon weight will be deposited on the local grid element. The amount deposited ΔW is computed as follows:

$$\Delta W = W \sigma_a / \sigma_t \tag{12}$$

The total weight $A(r, z)$ accumulated at the local grid element is updated by adding the deposited weight ΔW :

$$A(r, z) \leftarrow A(r, z) + \Delta W \tag{13}$$

The photon weight can then be decremented as follows:

$$W \leftarrow W - \Delta W \tag{14}$$

The next event that happens to the photon packet after absorption is scattering. The deflection angle $\theta \in [0, \pi)$ and the azimuthal angle $\psi \in [0, \pi)$ will be sampled statistically. The probability function for the cosine of the deflection

angle, $\cos \theta$ is described by the Henyey - Greenstein scattering function:

$$p(\cos \theta) = \frac{1 - g^2}{2(1 + g^2 - 2g \cos \theta)^{3/2}} \quad (15)$$

where g is the anisotropy factor, $g \in (-1, 1)$. A value of 0 indicates isotropic scattering and a value near 1 indicates strong forward scattering. Values of g range from 0.3 to 0.98 for human tissues. The choice of $\cos \theta$ can be expressed as a function of the random number ξ :

$$\cos \theta = \begin{cases} \frac{1}{2g} \left\{ 1 + g^2 - \left[\frac{1 - g^2}{1 - g + 2g\xi} \right] \right\} & \text{if } \xi \leq 1/m \\ 2\xi - 1 & \text{if } \xi > 1/m \end{cases} \quad (16)$$

Next, the azimuthal angle ψ , can be sampled from a uniform distribution over the interval 0 to 2π :

$$\psi = 2\pi \xi \quad (17)$$

The weight is decremented by the specular amount as it enters the tissue. The photon is then moved within the tissue. After taking a step, the photon weight is decremented due to absorption at the interaction site. Scattering occurs according to the Henyey-Greenstein phase function, P_{HG} , described in Section 3.

If the step size is large enough, the photon packet may hit a boundary. If the photon escapes from the upper boundary, the remaining weight will be recorded as diffuse reflectance. If it escapes from the lower boundary, it will be recorded as transmittance. Otherwise, if the photon hits a boundary at an angle greater than the critical angle, internal reflection may occur [9].

To decide if the photon is to be internally reflected or not, we compute the probability which depends on the angle of incidence α_i onto the boundary. The angle of incidence is calculated from the z component of the directional cosines:

$$\alpha_i = \cos^{-1}(|\mu_z|) \quad (18)$$

The internal reflectance, defined as the probability of a photon being internally reflected, is calculated by Fresnel's formulae using the following equation based on α_i :

$$R(\alpha_i) = \frac{1}{2} \left[\frac{\sin^2(\alpha_i - \alpha_t)}{\sin^2(\alpha_i + \alpha_t)} + \frac{\tan^2(\alpha_i - \alpha_t)}{\tan^2(\alpha_i + \alpha_t)} \right] \quad (19)$$

In cases where the photon packet is transmitted instead of internally reflected, Snell's law is used to find the angle of transmission α_t from the refractive indices that the photon is incident from n_i and transmitted to n_t using the following relation:

$$n_i \sin \alpha_i = n_t \sin \alpha_t \quad (20)$$

A photon packet can either be terminated naturally by reflection or transmission through the tissue. If the photon packet is still propagating in the tissue, and the photon weight W has been decremented sufficiently below a threshold level W_{th} , then further propagation is redundant. Proper termination has to be executed in order to ensure the conservation of energy without skewing the distribution of photon deposition.

A technique known as the roulette is used to terminate the photon packet when W falls below W_{th} . This technique gives the photon packet one chance in m of surviving with a weight of mW . If the photon packet does not survive the roulette, the photon weight is reduced to zero and the photon is terminated.

$$W = \begin{cases} mW & \text{if } \xi \leq 1/m \\ 0 & \text{if } \xi > 1/m \end{cases} \quad (21)$$

where ξ is a uniformly distributed pseudo-random number. This method terminates photons in an unbiased manner and thus conserves energy.

Figure 4 shows a summary of the whole process of Monte Carlo simulation of light transport. Although many other quantities like absorption, transmittance and fluence rate can be obtained from this simulation, we are mainly interested in the response of skin tissue to incident light coming from a range of angles, in the visible spectrum.

The main advantage of using the Monte Carlo method is that complex geometries and substrate information can be modelled to produce a variety of physical quantities. Actual optical and geometric properties of the materials can be used to influence the outcome of the simulation. The drawback is that it could be computationally expensive since many photon histories have to be traced to obtain physically accurate results.

6. RESULTS

Total reflection is made up of surface specular reflection and subsurface diffuse reflection. At near zero angle of incidence (i.e. angle between normal and incident ray is zero), total reflectance is dominated by diffuse components. Specular surface components dominate the reflectance properties at glancing angles of incidence. The overall effect is a smoothing of the reflection, producing a complex behaviour.

The BRDF measures the ratio of the exiting radiance to the incident irradiance on an opaque surface at a given point. To verify the physical accuracy of the model, we have compared the resultant BRDF with 2 publicly available datasets: the measured BRDF of human skin (Sample 39) from the Columbia-Utrecht Reflectance Database [4] and the image-based BRDF measurement of human skin by Marschner et al [5][15]. Dana et al have acquired the reflectance of a human skin sample, by removing the skin from the cadaver and preparing it into a flat sample. It was mounted on a positioning device to ensure stability for the time needed to gather the BRDF information. Measurement of the reflectance function was done using a video camera

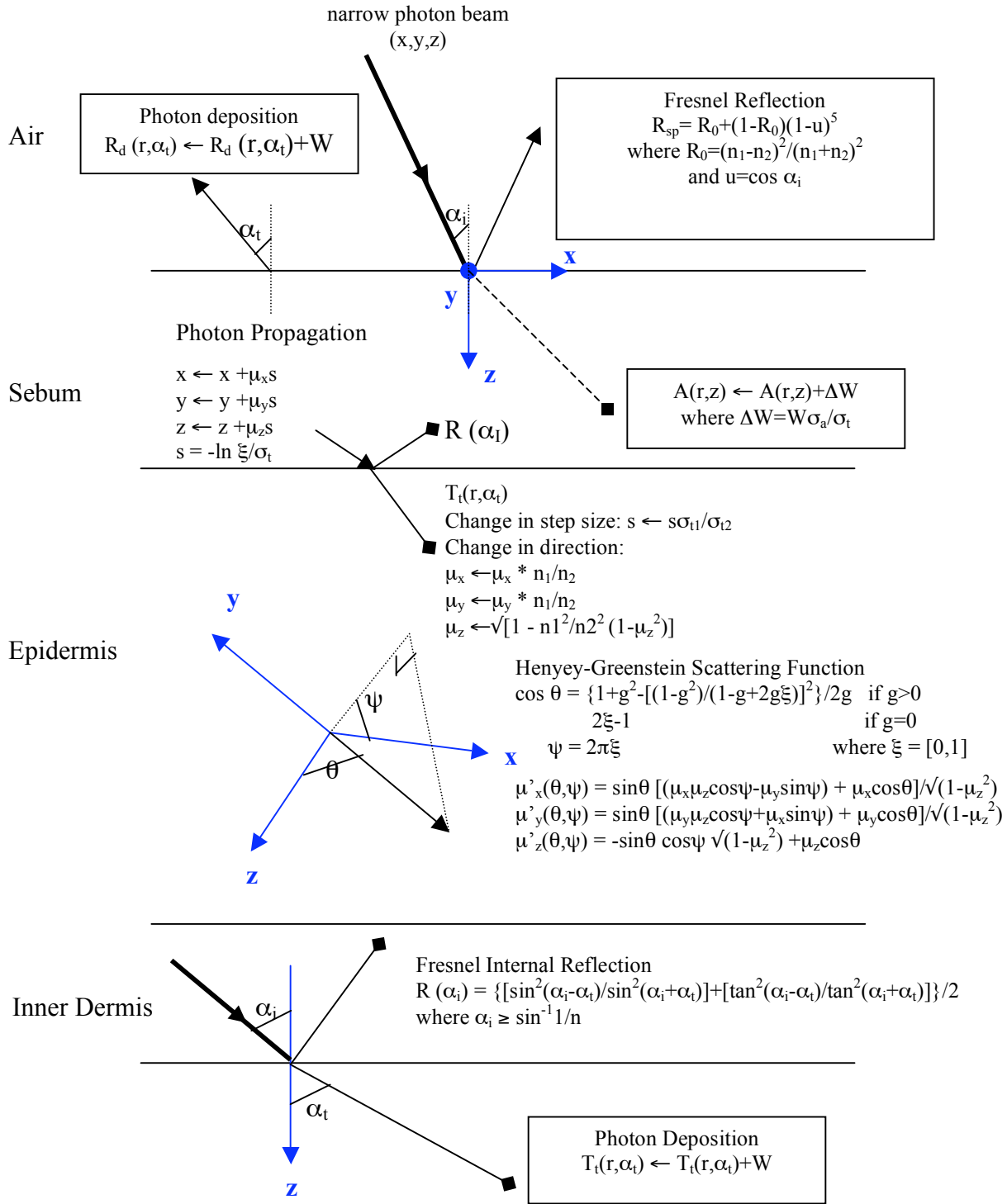


Figure 4. Monte Carlo Modelling of Light Transport in 3-layer Skin –Physical Equations

and robot. Marschner et al have measured the BRDF of living human skin using an image-based technique that derives the positions and orientations of a convex part of the body from a series of photographs [5].

The BRDFs are shown in Figure 5, where the solid red line represents our simulated subsurface BRDF, the dashed blue line represents the Columbia-Utrecht measured BRDF and the dotted green line represents the reflectance measurements by Marschner et al.

By varying the incident angle, it can be seen from the shape of the graphs that reflectance is dominated by subsurface diffuse component at near perpendicular angles and Fresnel surface reflection at glancing angles. For a low angle of incidence of 11 degrees, the three BRDFs are very

similar. The new subsurface reflectance fits the Marschner BRDF obtained from living skin very well. Deviations can be found at higher angles of incidence. Even the two sets of experimental data from Marshner and Columbia-Utrecht vary considerably at 78 degrees. This can be due to several factors. Natural variations in epidermal melanin pigmentation of the skin samples could contribute to the differences in scattering and absorption properties. Besides, the skin sample used for Columbia-Utrecht BRDF measurement was removed from a cadaver, which will have different levels of hydration and blood from living skin. Other sources of variation could be the lighting conditions as well as different levels of hydration, which influence the surface reflectance of the skin.

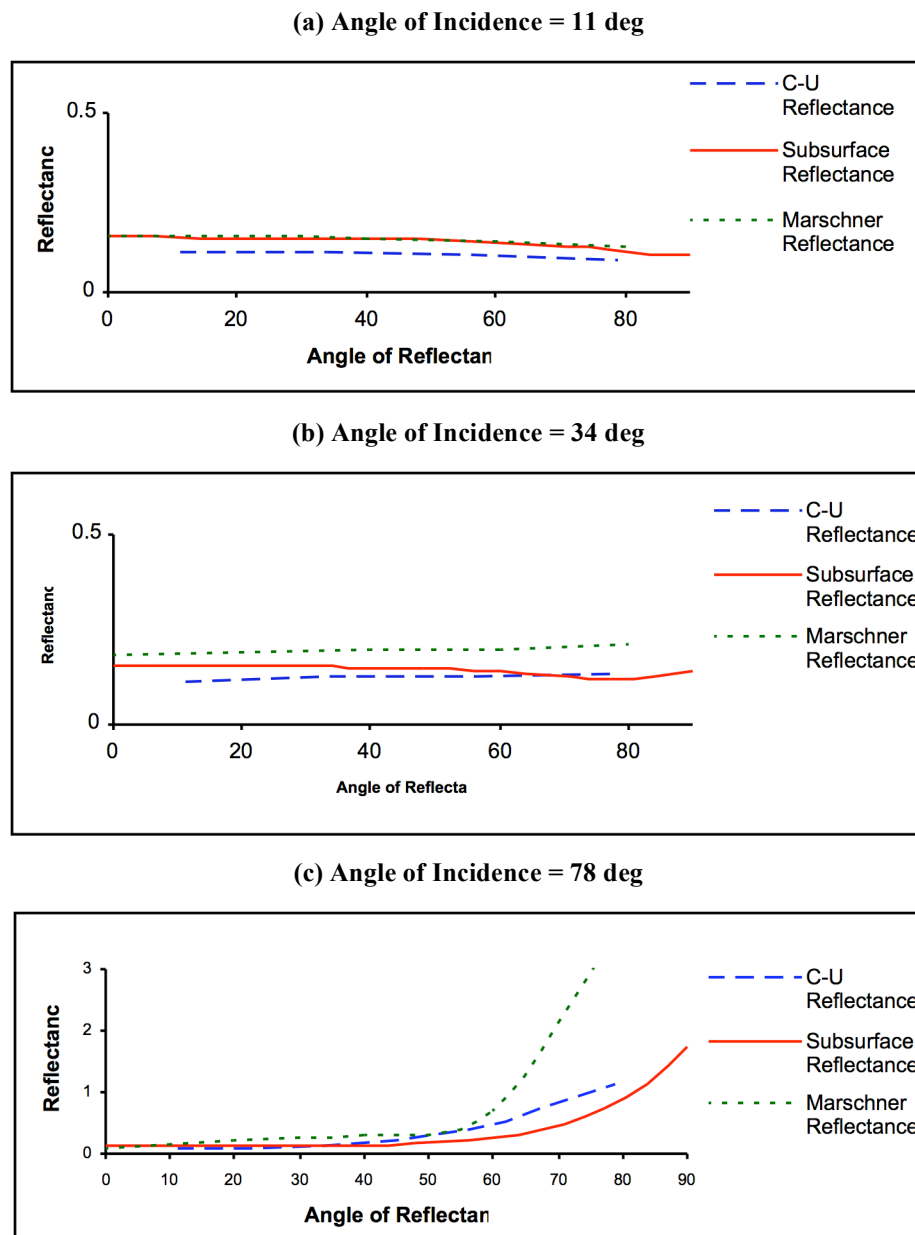


Figure 5. Comparison of Subsurface Reflectance (red solid line) with Columbia Utrecht Reflectance Database Sample 39 of Human Skin (dashed blue line) and Marschner's human skin BRDF measurement (dotted green line)

The effect of the sebum layer can be clearly shown in Figure 6. The refractive index for the thin sebum layer is higher than that of the epidermis; it is assigned a value of 1.5. Figure 6(a) does not have a layer of facial oil and appears to be matte and dry. A layer of sebum is applied in Figure 6(b) results in a less perfect but natural oily complexion with a shiny forehead.

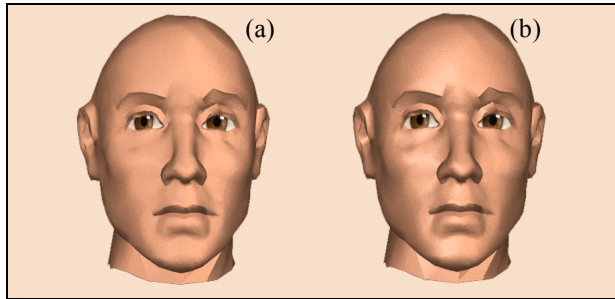


Figure 6. Effect of Sebum Layer
(a) Without Sebum
(b) With layer of sebum

The subsurface shading model is compared to conventional shading models in Figure 7. Each shading model is applied uniformly to the entire skin surface of the head. Figure 7(a) was rendered using Phong shading. The surface shows very strong highlights at areas where light strikes the surface at normal incidence, producing a very “plastic” appearance. Figure 7(b) shows the result of Lambert shading, where light is scattered isotropically. A very chalky appearance is produced, due to very little variation in intensity across the skin surface. Subsurface shading is used in Figure 7(c). There is greater accentuation and variation in shading due to the directional scattering of light from the Monte Carlo simulation, producing a more natural and smooth appearance. Subtle highlights indicate the presence of sebum on the face.

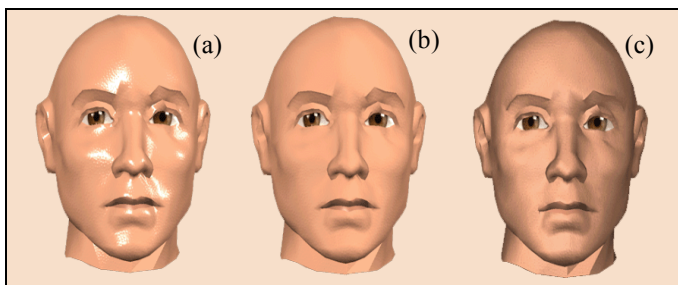


Figure 7. Comparison with other shading models
(a) Phong shading
(b) Lambert shading
(c) Subsurface shading

Surface texturing is a very important part of visual realism of the simulated skin surface. When skin is observed closely, it depicts a few types of micro structures. One

common type of micro pattern comprises of many random dots, otherwise known as pores that are commonly found on the face. Bump mapping is used to render the pores on the skin surface. Figure 8 shows a close-up image of the synthetic man’s head with an imperfect complexion. The head is rendered using the subsurface reflection model.

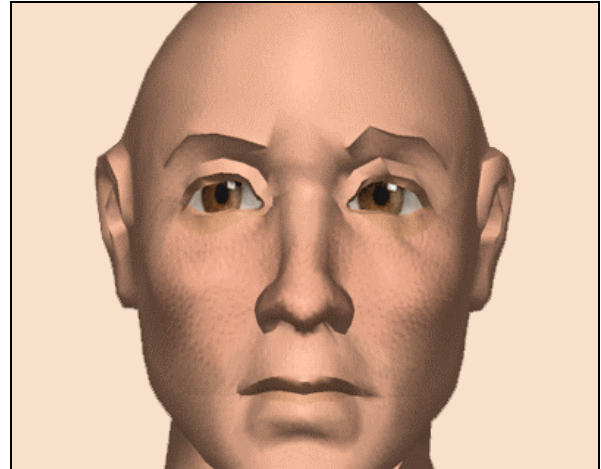


Figure 8. A synthetic human head with texture

Human skin found on other parts of the body can also be similarly rendered using the new subsurface reflectance model with other types of micro-textures. Another common micro-texture resembles a pattern with a net-like structure and consisting of mostly triangles as shown in Figure 9(a). The edges of the triangular forms define the location of micro lines or furrows and the curved surface surrounded by furrows defines the ridges. Figure 9(b) shows a rendered image of the skin texture from the triangulation. The texture can be tiled seamlessly without any visible boundaries.

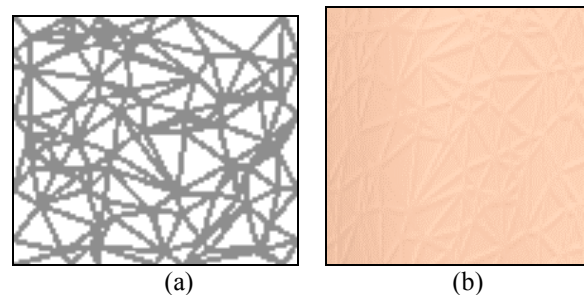


Figure 9. Net-like micro-texture and the rendered image

The geometrical patterns on the back of the hand and other parts of the body formed by the furrows of the skin can be specifically modelled by defining a set of random points and subsequent Delaunay triangulation. The points are spread across the whole surface to create a seamless procedural texture surface. Figure 10 shows the result of rendering a synthetic hand using the subsurface reflection model and additional texturing and bump mapping.

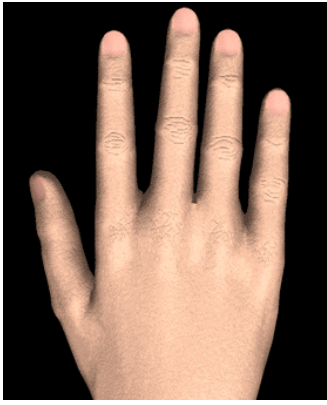


Figure 10. Synthetic human hand

7. CONCLUSION

Reflectance modelling is a difficult challenge with many competing constraints. We have adopted a theoretical approach based on skin optics principles as this method is less expensive compared to measurement-based methods, which requires specialised equipment and specially prepared samples. Our approach is highly flexible as it can be customised and spatially varied to produce a wide variety of multi-layered surfaces. It can be applied to many other industries where physical accuracy of reflection simulation models is essential.

The multi-layered reflection model performs a Monte Carlo simulation, which traces photon propagation in a three-layer skin model, including a layer of sebum, which is commonly found in varied amounts on the surface of human skin. This layer is previously neglected in skin reflection models, even though it contributes greatly to the surface appearance. Sebum is explicitly modelled to produce a more realistic and natural skin appearance.

The diffuse component varies directionally and is influenced by optical and geometric properties of the human skin. These properties have been directly calculated from experimental data in skin optics research. The inverse relationship between the diffuse and specular components is not captured in the traditional Lambertian reflection model. Unlike Hanrahan's work [8], which has not been experimentally verified, we have compared our simulation results with measured reflectance data from the Columbia-Utrecht Reflectance Database and Marschner et al, and found them to be highly similar.

References

- [1] Nikolaos Gazepidis and Dimitrios Rigas (2008) "Evaluation of Facial Expressions and Body Gestures in Interactive Systems", International Journal of Computers. Vol. 2 No. 1. Pg. 92~97.
- [2] Gonzalez A., Ferrer M. A., ALONSO, J B Travieso C M, "TDS: The software for the early diagnosis of melanoma", the 4th WSEAS International Conference on Information Security, Communications and Computers, Tenerife, Spain, December 2005. Pp. 365-368.
- [3] Gemert Van, M.J.C., Jacques S.L., Sterenborg, H.J.C.M., Star, W.M (Dec. 1989), "Skin optics", IEEE Transactions on Biomedical Engineering 36, 12, pp. 1146-1154.
- [4] Dana K.J., Ginneken B., Nayar S.K. and Koenderink J.J. (1999) "Reflectance and Texture of Real World Surfaces", ACM Transactions on Graphics, 18(1), pp. 1-34.
- [5] Marschner S. R., Westin S. H., Lafortune Eric P. F., Torrance Kenneth E., and Greenberg Donald P. (1999), "Reflectance Measurements of Human Skin", Eurographics Workshop on Rendering.
- [6] He X. D., Torrance K. E, Sillion F. X. and Greenberg D. P. (1991), "A comprehensive physical model for light reflection", Computer Graphics, 25(4), pp. 175-186.
- [7] Oren Michael and Nayar S. K. (1994), "Generalization of Lambert's Reflectance Model", ACM Computer Graphics Proceedings, Siggraph '94, pp. 239-246.
- [8] Hanrahan P. and Krueger W. (1993), "Reflection from Layered Surfaces due to Subsurface Scattering", SIGGRAPH '93 Conference Proceedings, Anaheim, California, pp. 165-174.
- [9] Wang L. and S. L. Jacques, "Monte Carlo Modelling of Light Transport in Multi-layered Tissues in Standard C", Computer Methods and Programs in Biomedicine, 47, pp. 131-146, 1995.
- [10] Schlick C. (1994), "An Inexpensive BRDF Model for Physically-based Rendering", Eurographics '94, Computer Graphics Forum, 13(3), pp. 233-246.
- [11] H. Zeng, H. Lui, C. MacAulay, D.I. McLean, B. Palcic, "Optical Spectroscopy for Skin Cancer Diagnosis", Available at http://bccancer.bc.ca/research/imaging/to01_title.html.
- [12] Jacques S.L (Jan. 1998), "Skin Optics", Oregon Medical Laser Center News.
- [13] Moritz Störing, Hans J. Anderson and Erik Granum, "Skin colour detection under changing lighting conditions", 7th Symposium on Intelligent Robotics Systems, Coimbra, Portugal, 1999.
- [14] Fiala P., Kadlecova E., "Progressive Methods in the Numerical Modeling by the Finite Elements", 7th WSEAS International Conference on Automatic Control, Modeling and Simulation (ACMOS '05), Prague, Czech Republic, March, 2005
- [15] Martin K. (1999), "Infrared and Raman Studies of Skin and Hair: A review of cosmetic spectroscopy", The Internet Journal of Vibrational Spectroscopy, 3(2), <http://www.ijvs.com/volume3/edition2/section2.htm>, Perkin-Elmer.